Received: 28 March 2021 | Revised: 9 November 2021 | Accepted: 15 November 2021

DOI: 10.1111/mec.16290

ORIGINAL ARTICLE

MOLECULAR ECOLOGY WILEY

Population subdivision promoted by a sea-level-change-driven bottleneck: A glimpse from the evolutionary history of the mangrove plant *Aegiceras corniculatum*

Rufan Zhang[1] | Zixiao Guo[1] | Lu Fang[1,2] | Cairong Zhong[3] | Norman C. Duke[4] | Suhua Shi[1]

[1]State Key Laboratory of Biocontrol, Guangdong Key Laboratory of Plant Resources, School of Life Sciences, Southern Marine Science and Engineering Guangdong Laboratory (Zhuhai), Sun Yat-sen University, Guangzhou, China

[2]Guangdong Provincial Key Laboratory of Biotechnology for Plant Development, School of Life Sciences, South China Normal University, Guangzhou, China

[3]Hainan Academy of Forestry (Hainan Academy of Mangrove), Haikou, China

[4]Centre for Tropical Water and Aquatic Ecosystem Research, James Cook University, Townsville, Australia

Correspondence
Zixiao Guo and Suhua Shi, State Key Laboratory of Biocontrol, Guangdong Key Lab of Plant Resources, Southern Marine Science and Engineering Guangdong Laboratory (Zhuhai), School of Life Sciences, Sun Yat-sen University, Guangzhou, China.
Email: guozx8@mail.sysu.edu.cn and lssssh@mail.sysu.edu.cn

Funding information
Guangdong Basic and Applied Basic Research Foundation, Grant/Award Number: 2021A1515011160; National Natural Science Foundation of China, Grant/Award Number: 31830005 and 31900200; National Key Research and Development Plan, Grant/Award Number: 2017FY100705; China Postdoctoral Science Foundation, Grant/Award Number: 2019M663212

Abstract

Historic climate changes drive geographical populations of coastal plants to contract and recover dynamically, even die out completely. Species suffering from such bottlenecks usually lose intraspecific genetic diversity, but how do these events influence population subdivision patterns of coastal plants? Here, we investigated this question in the typical coastal plant: mangrove species *Aegiceras corniculatum*. Inhabiting the intertidal zone of the tropical and subtropical coast of the Indo-West Pacific oceans, its populations are deemed to be greatly shaped by historic sea-level fluctuations. Using dual methods of Sanger and Illumina sequencing, we found that the 18 sampled populations were structured into two groups, namely, the "Indo-Malayan" group, comprising three subgroups (the northern South China Sea, Gulf of Bengal, and Bali), and the "Pan-Australasia" group, comprising the subgroups of the southern South China Sea and Australasia. Based on the approximate Bayesian computations and Stairway Plot, we inferred that the southern South China Sea subgroup, which penetrates the interior of the "Indo-Malayan" group, originated from the Australasia subgroup, accompanied by a severe bottleneck event, with a spot of gene flow from both the Australasia and "Indo-Malayan" groups. Geographical barriers such as the Sundaland underlie the genetic break between Indian and Pacific Oceans, but the discontinuity between southern and northern South China Sea was originated from genetic drift in the bottleneck event. Hence, we revealed a case evidencing that the bottleneck event promoted population subdivision. This conclusion may be applicable in other taxa beyond coastal plants.

KEYWORDS
Aegiceras corniculatum, bottleneck, coastal plant, mangrove, phylogeography, population subdivision

1 | INTRODUCTION

Many coastal plants disperse propagules by seawater. Therefore, geographical barriers such as landmasses, open oceans (Thornhill et al., 2008), and ocean currents (Guo et al., 2016; Pil et al., 2011; Wee et al., 2014), constrain the margins of their distribution range. These barriers also cause abrupt discontinuities within the ranges of coastal plants (Hartl & Clark, 1997). Moreover, limitations of

dispersal ability may further shape their populations, following a pattern called isolation by distance (IBD), which assumes that the level of differentiation is positively correlated with geographic distance.

The geographic and ecological landscapes of coastal regions are not persistent throughout history, making the populations of coastal plants highly dynamic. Geological actions change the geographical landscape gradually in a macroevolutionary timescale, such as the closure of the Central America isthmus (Lessios, 2008). In a smaller timescale, the historic sea-level changes cause geographic barriers to emerge and vanish repeatedly. The emergence of a barrier may subdivide populations while the vanish of a barrier may reunite diverging populations (Ge et al., 2015). Hence, the population structure within a species is an integrated output of the forces dividing populations and those mixing populations.

Other than isolating and connecting populations, historic geographical and climatic changes also shape the population size of populations. Typically, the populations of a species contract to refugia or even become extinct when geographic or ecological conditions are too hostile to survive (Foufopoulos et al., 2011; Hallam & Wignall, 1999; Paulay, 1990), and recover and expand when the conditions are mild. When a species survives through a bottleneck event, it commonly suffers from loss of the majority of its polymorphisms in the "shrinkage" process (Haanes et al., 2010; Mamuris et al., 2005; Moum & Árnason, 2001; Tsuchida et al., 2014). In addition to reducing intraspecific diversity, such bottleneck events are potent to generate novel genetic structures within species. Such potential may source from three mechanisms. First, different alleles may be retained among refugial populations, and the retained alleles are highly likely to be fixed. Second, due to intensified genetic drift, newly emerging alleles in the refuge population are more likely to be fixed. Third, the exchange of alleles between populations is unlikely because barriers between refuge populations are usually strong.

Several previous studies have related bottleneck events to genetic structures indirectly. In a coral reef fish, the strong nonequilibrium genetic structure was shown to be generated by genetic bottlenecks/founder effects associated with population reduction/extinctions and asymmetric migration or recolonization (Bay et al., 2008). Repeated bottleneck events during colonization of the parasite *Geomydoecus aurie* have been shown to impact the genetic structure of a population due to allele surfing (Demastes et al., 2019). The fine-scale genetic structure of *Rhizophora racemosa* in the Cameroon estuary complex was attributed to contemporary processes such as restricted propagule dispersal, bottleneck events, and recolonization by founders from ancient local refugia (Ngeve et al., 2017). Despite the awareness that bottlenecks may generate genetic structure, the hypothesis needs to be comprehensively and explicitly addressed. The model with which to test this hypothesis should live in a highly dynamic habitat and be sensitive to habitat change.

Mangroves, a group of typical coastal plants, are therefore an ideal model. Mangrove plants are distributed linearly along coasts and strictly inhabit tropical and subtropical intertidal zones. In the Quaternary cycles of glacial and interglacial conditions, climate changes drove the sea level to change in cycles (Miller et al., 2005; Zachos et al., 2001). The coastlines shifted following the sea-level rise and drop, and mangrove forests were forced to advance and retreat repeatedly (Woodroffe & Grindrod, 1991). Several studies have determined the genetic structure of different mangrove species, with periodic geographical barriers frequently identified in places such as the Malay Peninsula and the Wallacea region (Guo, Guo, et al., 2018; Guo et al., 2016; Li et al., 2016; Urashi et al., 2013; Yang et al., 2016, 2017), in addition to a set of permanent barriers (Duke, 2017). The periodic erosion of geographical barriers resulted in intermittent gene flow, which shaped the population divergences and admixtures of many coastal species (Banerjee et al., 2020, 2021; Guo, Guo, et al., 2018; Guo et al., 2016; Westberg & Kadereit, 2009). Previous studies also revealed that bottleneck events, which resulted from the fluctuations in sea level, have caused population diversity reduction in some species (Guo et al., 2020; Guo, Ng, et al., 2018; Zhou et al., 2010). However, there has been no study that tests the hypothesis bottleneck events promote population subdivision. *Aegiceras corniculatum* is a typical mangrove species. It shows a high level of genetic differentiation between populations in Hainan and the Gulf of Thailand, regardless of the low genetic diversity within each region (Guo, Li, et al., 2018). Therefore, *Ae. corniculatum* provides an ideal model to test the hypothesis, probably by a comprehensive phylogeographic study.

Ae. corniculatum distributes widely from India across Southeast Asia and South China to Australia and west Pacific islands (Duke, 2014), probably facilitated by its long-distance dispersal via buoyant propagules. However, the patterns of the genetic structure of *Ae. corniculatum* are only available in local regions of China, the Malay Peninsula, and Sri Lanka from two previous studies (Deng et al., 2009; Ge & Sun, 1999), hindering our understanding of the species-wide pattern across its range. One previous study using inter-simple sequence repeat markers found low genetic diversity and population differentiation of *Ae. corniculatum* in China (Ge & Sun, 1999), and the other one using amplified fragment length polymorphism markers revealed geographical grouping of genetic variations into China, Malay Peninsula, and Sri Lanka (Deng et al., 2009). To ascertain the population structure of *Ae. corniculatum* across its distribution range, we sampled 18 populations covering the range and used both Sanger and Illumina sequencing to obtain single nucleotide polymorphism (SNP) markers. With this data, we expect to test the hypothesis that bottleneck events could promote population subdivision by observing that: (1) the populations of *Ae. corniculatum* from the Indian Ocean, Southeast Asia (including South China), and Australasia are exclusively grouped; (2) the historic sea-level changes have resulted in bottleneck events in the demographic history of *Ae. corniculatum* populations; (3) such historic bottleneck events play a role in generating additional population structure not attributed to geographic barriers.

The findings would deepen our understanding of population evolution in dynamic geographic and climate changes. This evolutionary insight would first provide instructions for the communities of mangrove conservation and management worldwide. Mangroves are of high value in supporting coastal ecosystems and protecting coasts

(Barbier, E. B., 2011), but they are vulnerable to the projected sea-level rise (Guo, Li, et al., 2018). The insights from *Ae. corniculatum* would guide the global efforts to conserve the intraspecific genetic diversity of all mangrove species. Moreover, although we focus on coastal plants, the underlying reasonability may be general in other taxa, for example, species in fragmented habitats, invasive species, and introduced species. Many plants and animals may involve in such processes, especially upon the intensifying global climate changes and anthropogenic disruptions.

2 | MATERIALS AND METHODS

2.1 | Plant materials and sequencing

From 2009 to 2013, a total of 631 *Ae. corniculatum* individuals from 18 sites in the Indo-West Pacific region were collected (Figure 1a, Table 1). The sampled individuals were at least 5 m apart, and one fresh leaf was collected from each individual. Sampled leaves were preserved in plastic bags with silica gel. DNA of each individual was extracted using the cetyltrimethylammonium bromide (CTAB) method (Allen et al., 2006).

Referencing the transcriptome of an individual from Hainan, we designed a set of primers anchored at the nuclear genome of *Ae. corniculatum*, with each pair of primers anchoring at exons but spanning at least one intron. We selected 93 pairs of new primers to use in this study based on two criteria: the primer is successfully amplified in the population samples and it produces amplicons of 200–2,500 bp long.

As the sequences for each individual can be explicitly obtained through Sanger sequencing, we sequenced a partial of samples from all the 18 populations in six genes to get a complete view of the population genetic pattern. Six genes (A189, A245, A383, A414, A440, and C058) were randomly selected to amplify in 10 to 37 individuals from the 18 populations (423 in total) (Figure 1, Table 1). The amplicons were sequenced using the Sanger method on an ABI 3730 platform at Huada Genomic Institute (BGI) (Shenzhen). The PCR procedure for amplification was as follows: 4 min at 94°C; 30 cycles of 15 s at 94°C, 15 s of annealing at 53°C, and extension at 72°C for 2 min; and a final 10 min extension at 72°C. The reactions were held at 10°C before the PCR products were subjected to electrophoresis on 1% agarose gels.

Limited by the cost and workload of PCR amplification and sequencing, the Sanger sequencing was inefficient to sequence a large number of individuals and genetic markers. Hence, we used a pool-sequencing strategy to sequence all 93 genes against 11 populations (491 individuals in total) on a high-throughput Illumina GA platform at Huada Genomic Institute (BGI) (Shenzhen). The mutual corroborations of the two sets of data convincingly validated the revealed pattern. For each population, we pooled equal amounts of DNA

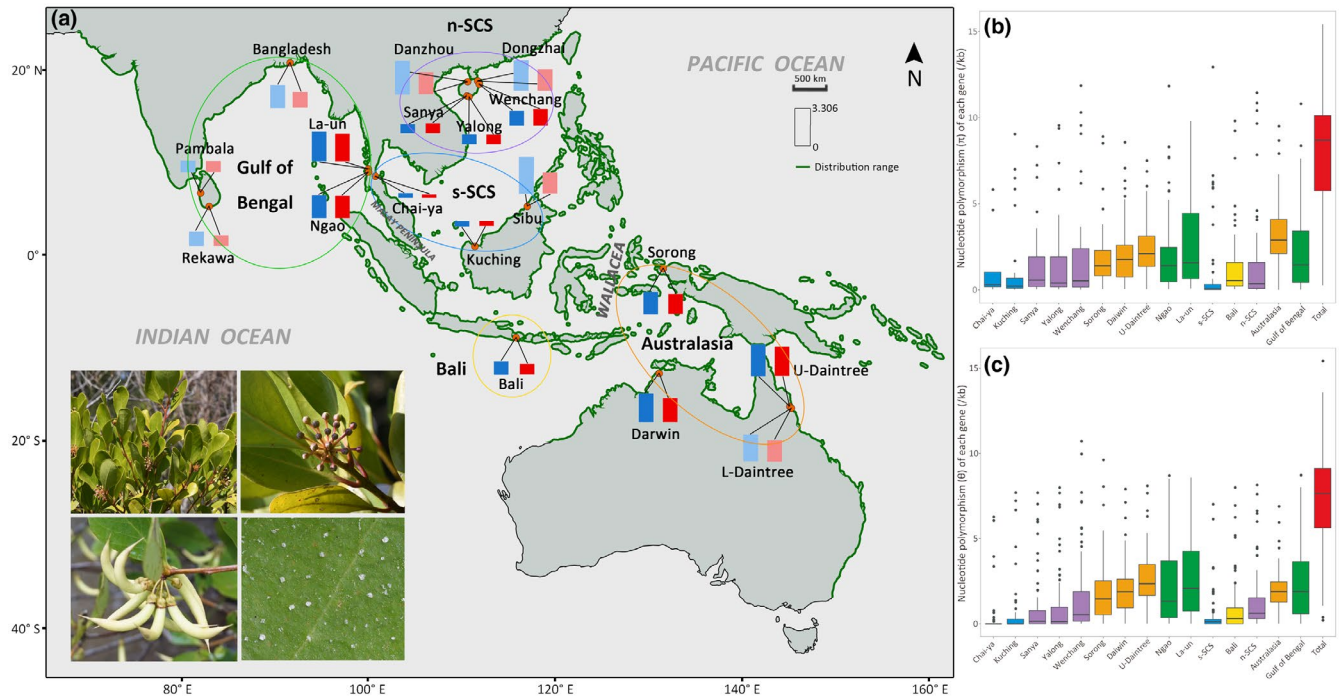

FIGURE 1 Population genetic diversity of *Aegiceras corniculatum*. (a) Distribution of π and θ across 18 populations (per kb). The height of the rectangle is proportional to the levels of π and θ. Blue is π, and red is θ. Dark red/blue bars indicate values obtained from Illumina data while light red/blue ones indicate values obtained from Sanger data. (b) Boxplots of the π of each gene across 11 Illumina-sequenced populations (per kb). (c) Boxplots of the θ of each gene across 11 Illumina-sequenced populations (per kb). Boxes of the same colour indicate populations in the same geographical area. As indicated by the circle in (a), green, blue, purple, yellow, and orange indicate "Gulf of Bengal", "s-SCS", "n-SCS", "Bali", and "Australasia", respectively. "Total" indicates the genetic divergence of *Aegiceras corniculatum* at the species level

TABLE 1 Basic information of population sampling of *Aegiceras corniculatum*

Site ID	Location	Longitude and latitude	Sequencing platform	Sample size[†]
Sanya	Sanya, Hainan, China	18°14'N, 109°30'E	Sanger & Illumina	24(24)
Wenchang	Wenchang, Hainan, China	19°36'N, 110°47'E	Sanger & Illumina	24(100)
Yalong	Yalong Bay, Hainan, China	18°13'N, 109°36'E	Sanger & Illumina	24(50)
U-Daintree	Upper Daintree River, Australia	16°16'S, 145°18'E	Sanger & Illumina	24(40)
Darwin	Darwin, Australia	12°28'S, 130°51'E	Sanger & Illumina	24(42)
Sorong	Sorong, West Papua, Indonesia	0°52'N, 131°15'E	Sanger & Illumina	22(22)
La-un	La-un, Thailand	10°10'N, 98°43'E	Sanger & Illumina	33(36)
Ngao	Ngao, Thailand	09°52'N, 98°36'E	Sanger & Illumina	37(51)
Kuching	Kuching, Malaysia	1°34'N, 110°21'E	Sanger & Illumina	23(40)
Chai-ya	Chai-ya, Thailand	9°23'N, 99°16'E	Sanger & Illumina	24(50)
Bali	Bali, Indonesia	8°43'S, 115°19'E	Sanger & Illumina	24(36)
Danzhou	Danzhou, Hainan, China	19°26'N, 109°34'E	Sanger	24
Dongzhai	Dongzhai harbor, Hainan, China	19°58'N, 110°34'E	Sanger	27
Bangladesh	Bangladesh	22°1'N, 89°46'E	Sanger	22
Pambala	Pambala, Sri Lanka	7°30'N, 79°50'E	Sanger	11
Rekawa	Rekawa, Sri Lanka	6°3'N, 80°51'E	Sanger	10
Sibu	Sibu, Malaysia	6°2'N, 116°7'E	Sanger	22
L-Daintree	Lower Daintree River, Australia	16°17'S, 145°27'E	Sanger	24

[†]The numbers outside brackets are individual number for Sanger sequencing while those inside brackets are number for Illumina sequencing.

from all the individuals of the population. For each of the 93 genes, we amplified the pooled DNA using the same procedure described above, and the purified PCR products of all 93 nuclear loci from one population were further pooled in equal quantities to reach a total of 10 μg for sequencing.

2.2 | Sequence analysis and genetic diversity estimation

The sequences of 18 populations obtained from Sanger sequencing were aligned and edited in SeqMan 7.1.0. For each population, the nucleotide diversity (π) and DNA polymorphism (Watterson's θ) were calculated using DnaSP 5.10 (Librado & Rozas, 2009).

We obtained the reference sequences of the 93 genes by sequencing one *Ae. corniculatum* individual using the Sanger method (see the supporting information file of He et al., 2019). The reference sequences ranged in length from 203 to 2,422 bp. The short reads produced from Illumina sequencing were mapped to reference sequences using MAQ 0.7.1 (Li et al., 2008) with the parameters set such that the mutation rate between the reference and read was 0.002, the threshold of mismatch base quality sum was 200, and the minimum mapping quality of the reads was 30. To exclude false-positive mismatches, we counted the mismatch rate for each site across the read and the mismatch rate for each base quality. We trimmed the first and last 10 bases of each read and filtered bases with a quality score of less than 20. Single nucleotide polymorphisms (SNPs) were also identified using MAQ 0.7.1 (Li et al., 2008). To avoid introducing bias from sequencing errors, we discarded the sites with insufficient site coverage (<100 reads) and those with minor allele frequency less than 1/2N (N is the number of individuals) in each population (He et al., 2013). The allele frequencies for each SNP site in a population were obtained by counting the depth of each allele.

For the Illumina data, we estimated the nucleotide polymorphism (Watterson's θ) of each gene using the method of He et al. (2013). The nucleotide diversity (π) of each gene was also estimated according to Nei's formula (Nei, 1987) with an in-house script (the script is available upon request). To estimate absolute genetic divergence between populations, we computed pairwise D_{XY} following the formula derived by Nei (Nei & Li, 1979). Pairwise D_{XY} values were summed over all SNPs, and the sum was normalized by effective sequence length. For each pair of populations, the effective sequence length was defined by sites without missing data in either population. We also estimated Wright's F statistics (F_{ST}) (Wright, 1950) with these data.

2.3 | Inferring population structure

To identify the genetic structure of *Ae. corniculatum*, 423 individuals from 18 populations with Sanger sequences were assigned into a putative number of clusters using a Bayesian clustering approach with STRUCTURE 2.3.4 (Falush et al., 2003; Hubisz et al., 2009; Pritchard et al., 2000). The program identifies the K genetic clusters of origin of the sampled individuals and assigns the individuals simultaneously to the genetic clusters by calculating the posterior probability.

The maximum K was set to 12, and for each K, 10 replicates were conducted. Each run consisted of 1×10^6 Markov chain Monte Carlo (MCMC) iterations with a burnin of 2×10^5 under an assumed model of admixture and correlated allele frequencies. The most likely K was determined by the delta K statistic using STRUCTURE HARVESTER (Evanno et al., 2005). The population structure results are shown graphically by DISTRUCT 1.1 (Rosenberg and a., 2004), and each individual is a line segment partitioned into K coloured components, which represent the individual's estimated membership coefficients in the K clusters.

We also performed principal component analysis (PCA) on the SNP frequency matrix (summarizing the frequency of each SNP in each Illumina-sequenced population) using the princomp function in R (Venables & Ripley, 2013) to test whether the SNP frequencies differed among populations. Using the pegas R package, the analysis of molecular variance (AMOVA) was performed to characterize the hierarchical assignment of variance components at levels of population and cluster of populations. We performed this analysis for each of the six Sanger-sequenced genes.

The revealed genetic structure was further checked gene by gene by constructing a haplotype network for each gene and mapping the haplotypes geographically. Haplotypes of six nuclear genes across the 18 populations were inferred using DnaSP 5.10 (Librado & Rozas, 2009), and the networks were constructed by an expectation-maximization algorithm with *Ae. floridum* as the outgroup. The networks were visualized using NETWORK 5.0 (http://www.fluxus-engineering.com/) (Bandelt et al., 1999) and plotted on a map using GenGIS (Parks et al., 2009).

The 93 genes sequenced by the Illumina platform were also used to infer haplotypes using the method developed by (He et al., 2019). He et al. validated the accuracy of this method to infer haplotypes by sequencing individuals using the Sanger method. The details associated with using this method have been described in a previous publication (Wang et al., 2021). We obtained 392 gene segments, among which 84 gene segments were longer than 300 bp. Haplotype network was also constructed for each segment longer than 300 bp using NETWORK 5.0 (http://www.fluxus-engineering.com/) (Bandelt et al., 1999).

2.4 | Inferring geographical barriers

To identify the biogeographical boundaries that exhibit the largest genetic discontinuities between population pairs, we used the F_{ST} matrix as the distance matrix to calculate the Monmonier maximum difference by BARRIER 2.2 (Manni et al., 2004). To ensure robustness, we randomly selected 30 genes from the 93 genes to accumulate one F_{ST} matrix. We repeated this process 100 times and obtained 100 F_{ST} matrices. The robustness of each barrier was assessed by bootstrapping over the 100 matrices of genetic differentiation.

Mantel tests of F_{ST} against geographic distance were performed to test the isolation by distance model. We used the spheric distance of pairwise sampling sites to approximate geographic distance. The test was conducted with 1,000 permutations and at two levels: all populations, and populations of a genetic group.

2.5 | Demographic history simulation

The populations were distinctly structured, according to the above-mentioned analyses. The populations in the southern South China Sea (Lineage 1, including Chaiya and Kuching) are closely related to those in Australasia (Lineage 2, including U-Daintree, Darwin, and Sorong) instead of those geographically surrounding them (Lineage 3, including Sanya, Wenchang, Yalong, La-un, Ngao, and Bali). To examine how the populations in the southern South China Sea originated, we built 12 models and used the approximate Bayesian computation (ABC) method to choose the optimal model. The 12 models were first different in population topology: (1) Lineage 2 diverged with Lineage 3 first and then Lineage 1 diverged from Lineage 3 (Models 1–4); (2) Lineage 2 diverged with Lineage 3 first and then Lineage 1 diverged from Lineage 2 (Models 5–8); and (3) Lineage 2 diverged with Lineage 3 first and then Lineage 1 derived from an admixture of Lineage 2 and Lineage 3 (Models 9–12). Within each topology, the four models differed in population reduction, population bottleneck, population reduction with gene flow, and population bottleneck with gene flow.

Simulated sequences under these models were produced by ms software (Hudson, 2002). To reduce the complexity of the parameters, we derived population size parameters from a single N_0. N_0 was randomly picked from the prior distribution and assigned to Lineage 1 as the baseline. The population size of the other two lineages (N_x) is equal to θ_x/θ_0, where θ_x and θ_0 are the observed θ of the current and baseline lineages, respectively. We performed 1×10^5 simulations using the ms program for each model (Hudson, 2002). Eighty loci of 1,000 base pairs were simulated in each run with the mutation rate set at 4.06×10^{-8} per generation per bp. The mutation rate was estimated from phylogenomic comparisons to closely related species (He et al., 2019). The sample size of each group was set equal to the corresponding cluster pooling in multiple populations. Uniform prior distributions were set for the demographic parameters, with corresponding parameters in different models having an identical prior range (Table S1).

For each simulation, we calculated 18 summary statistics, including Watterson's estimator (θ), nucleotide polymorphism (π), segregating sites (S), and Tajima's D within each group and D_{XY} and F_{ST} for each pair of groups. To perform model selection, we calculated Euclidean distances by comparing the summary statistics of the simulated and observed sequences. We set the tolerance as 0.05 to retain the simulated data, and then the approximate Bayesian computation schema (Beaumont et al., 2002) was used to estimate the Bayesian posterior probabilities of each mode using the abc package in R (Csilléry et al., 2012). The postpr function and neuralnet option were used. With the optimal model selected, the neuralnet method in the abc R package was again used to estimate the posterior distribution of demographic parameters.

To complement the results of ABC simulations, we also used Stairway Plot 2 (Liu & Fu, 2020) to reconstruct the dynamic history of population size (N_e) for the three lineages. The SNP information, which was obtained from the Illumina sequencing, was used to conduct this computation. We ran the program with suggested parameters according to the manual. The exception is that we set the mutation rate to 4.06×10^{-8} per generation per bp (He et al., 2019).

3 | RESULTS

3.1 | Genetic diversity of *Ae. corniculatum* at the population and species levels

Using Illumina sequencing techniques, we obtained 63 to 75 kb of DNA sequences covering 69 to 82 genes in the 11 populations (Table 2), ranging in length from 197 to 2,301 bp. The average sequencing depth of the Sanya, Wenchang, and Yalong populations was more than 2200 x, whereas that of the other eight populations was more than 4,400x. By mapping short reads to reference sequences, we identified 91 to 761 segregating sites within each population (Table 2). The π and θ for each Illumina-sequenced gene indicated a high level of genetic variation at the species level but relatively low genetic diversity within populations and regions (Figure 1b and c). Extremely low π and θ were observed in the populations Chai-ya and Kuching from the southern South China Sea, significantly lower than those in the Gulf of Bengal (La-un and Ngao, $p < .001$ for both π and θ, Wilcoxon test) and in Australasia (Sorong, Darwin, and U-Daintree, $p < .001$ for both π and θ, Wilcoxon test) (Figure 1, Table 2). The genetic diversity of Chai-ya and Kuching are also lower than those in Hainan Island, with significantly lower values of θ ($p < .001$, Wilcoxon test) but not π ($p = .026$, Wilcoxon test). The genetic diversity of populations without Illumina data was evaluated from the six nuclear genes sequenced by the Sanger method. Most of the populations from the northern South China Sea and Australasia have medium values of π and θ, and the two marginal populations in Siri Lanka composite a relatively low level of genetic variation (Figure 1, Table 2).

3.2 | Population structure within the distribution range of *Ae. corniculatum*

The Sanger sequences of 423 individuals from 18 populations were used to identify the uppermost hierarchical level of the genetic clusters. The optimal K was estimated to be two according to Evanno's method (Figure S1). One cluster included the Bali, La-un, Ngao, Bangladesh, Pambala, Rekawa, Dongzhai, Danzhou, Sanya, Wenchang, and Yalong populations, which cover almost the whole Asian range, except the southern South China Sea (Figure 2c). This cluster is defined as the "Indo-Malayan" group. The other cluster included the Kuching, Chai-ya, Sibu, U-Daintree, L-Daintree, Darwin, and Sorong populations, which cover the whole Australasia region and the southern South China Sea (Figure 2c). We call the second cluster the "Pan-Australasia" group.

To test whether a substructure exists within each group defined above, the same STRUCTURE clustering was applied to each group. The optimal K in the "Indo-Malayan" group was estimated to be four

TABLE 2 Genetic diversity estimation for 18 populations of *Aegiceras corniculatum*

Location ID	Analysed length (depth>100 bp)	Genes	SNPs	Polymorphic genes	$\theta(\times 10^{-3})$	$\pi(\times 10^{-3})$
Kuching	71,655	77	132	32	0.461	0.494
Chai-ya	72,314	78	91	11	0.298	0.412
La-un	63,098	69	639	65	2.491	2.703
Ngao	71,689	76	619	65	2.032	2.109
Sanya	64,323	75	209	37	0.893	0.834
Wenchang	75,214	82	524	59	1.507	1.347
Yalong	74,568	82	260	39	0.867	0.892
U-Daintree	70,890	77	761	76	2.652	2.885
Darwin	72,515	79	656	76	2.147	2.574
Sorong	74,228	81	479	67	1.798	2.023
Bali	73,564	78	291	50	0.944	1.208
Danzhou	4,494	6	39	6	1.973	2.948
Dongzhai	4,494	6	37	6	1.891	2.871
Bangladesh	4,494	6	26	5	1.373	1.921
Pambala	4,494	6	17	3	1.041	1.076
Rekawa	4,494	6	16	3	1.029	1.498
Sibu	4,494	6	33	2	1.788	3.259
L-Daintree	4,494	6	37	6	1.926	2.284

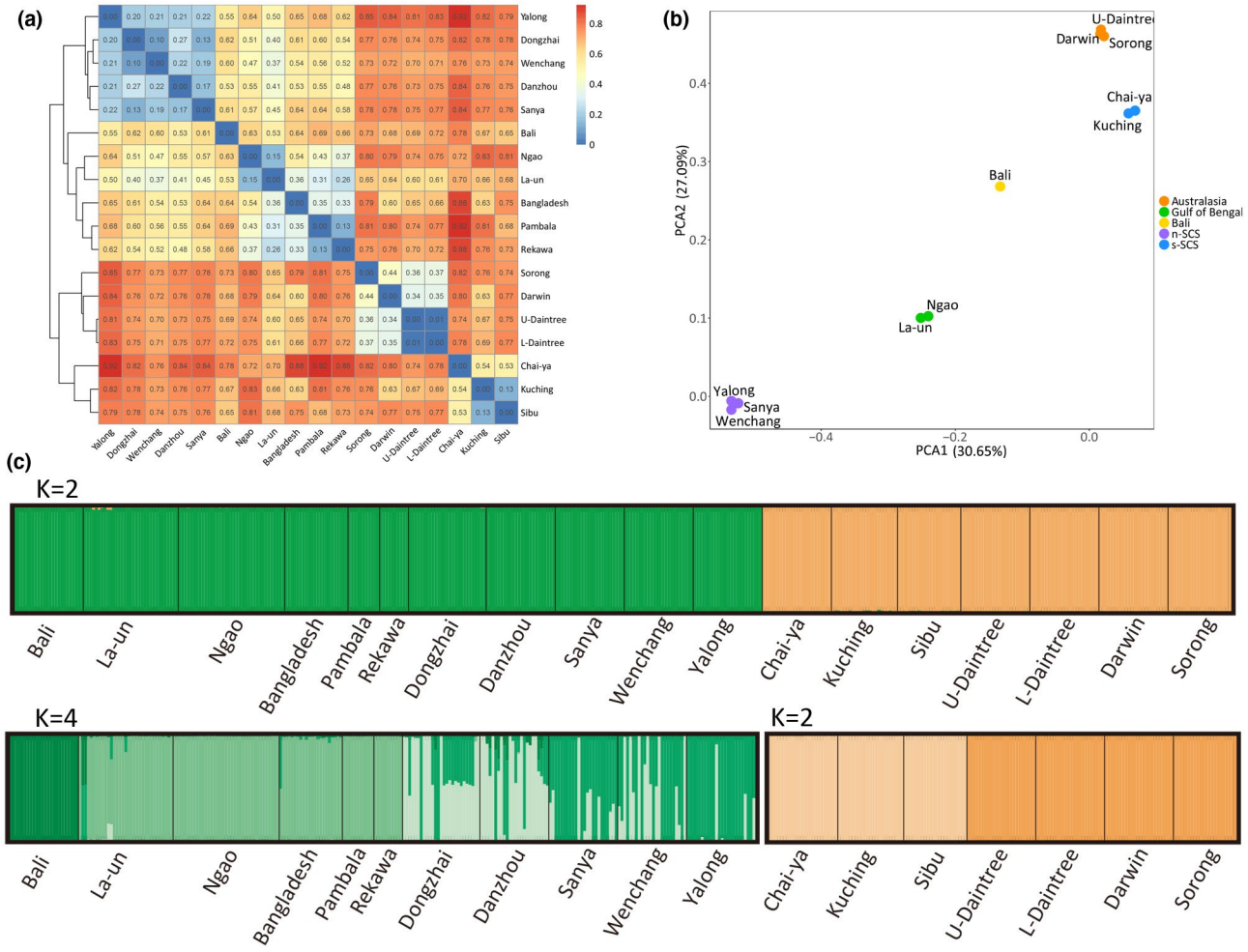

FIGURE 2 Genetic differentiation and structure of *Aegiceras corniculatum* populations. (a) Heatmap of the pairwise F_{ST} values of the 18 populations estimated from the six Sanger-sequenced genes. (b) Plot of the first and second axes of a principal component analysis based on the frequency of single nucleotide polymorphisms within each population of 82 deep sequencing genes. The letters are the site ID of the sampled populations. The colours of points indicate population clusters, that green, blue, purple, yellow, and orange indicate "Gulf of Bengal", "s-SCS", "n-SCS", "Bali", and "Australasia", respectively. (c) Bayesian clustering with STRUCTURE split the 18 populations of *Aegiceras corniculatum* into two groups (green indicates "Indo-Malayan" and orange indicates "Pan-Australasia"). Each group was further clustered into three (4) or two subgroups, which are coloured by different greens or oranges. Each thin vertical bar represents an individual, and each bold vertical bar separated by a black line represents a population. The population names are listed below the plot

according to Evanno's method (Figure S2). The populations around the Gulf of Bengal ("Gulf of Bengal" subgroup, including La-un, Ngao, Bangladesh, Pambala, and Rekawa) share a component, the single Bali population on Java Island ("Bali" subgroup) constitutes a component, and the remaining northern South China Sea populations ("n-SCS" subgroup, including Dongzhai, Wenchang, Danzhou, Sanya, and Yalong) consisted of two admixed components (Figure 2c). Hence, the "n-SCS" populations are more plausibly considered as one subgroup. In the "Pan-Australasia" group, two components (Figure S3) are distributed in the southern South China Sea ("s-SCS" subgroup, including Chai-ya, Kuching, and Sibu) and Australasia ("Australasia" subgroup, including U-Daintree, L-Daintree, Darwin, and Sorong) (Figure 2c). Hence, the 18 populations were reasonably clustered into two groups and further clustered into five subgroups.

The clustering pattern revealed by the Sanger sequencing data was validated using Illumina data. The PCA clustering based on the SNP frequency matrix revealed an approximately consistent pattern: (1) the "s-SCS" subgroup (represented by Kuching and Chai-ya) and "Australasia" subgroup (represented by U-Daintree, Darwin, and Sorong) grouped in the upper right corner; (2) the "n-SCS" populations (represented by Sanya, Yalong, and Wenchang) were grouped in the lower-left corner; and (3) the populations of the "Gulf of Bengal" (represented by La-un and Ngao) were grouped between the "n-SCS" population cluster and the single population ("Bali") (Figure 2b). Hence, the differentiation between the "Indo-Malayan" and "Pan-Australasia" groups is higher. Within the "Indo-Malayan" group, the "n-SCS" subgroup may be less different from the "Gulf of Bengal" subgroup than the "Bali" subgroup.

The F_{ST} and D_{XY} statistics provide a direct estimation of population differentiation and divergence. The F_{ST} values estimated from Sanger data agree well with the clustering pattern revealed above (Figure 2a). Both data sets show lower F_{ST} values between populations within each subgroup (ranging from 0.07–0.39 estimated from Illumina data and 0.01 to 0.54 from Sanger data), while higher F_{ST} values were observed between populations from different subgroups (0.42–0.53 from Illumina data and 0.37–0.92 from Sanger data) (Figure 2a and Figure S4). We performed the AMOVA to determine the hierarchical percentages of variation, based on the F_{ST} matrix of each of the six Sanger-sequenced genes. The majority of variation components (83.63%–97.20%) were attributed to "among subgroups" in all genes, except the gene A414 (40.13%) (Table S3). Consistently, little variation was attributed to "among populations within subgroup" or "within populations" (Table S3). The D_{XY} statistics estimated from the six Sanger-sequenced genes showed a very clear divergence between the five subgroups but an obviously lower divergence between populations within each subgroup (Figure S5). Interestingly, the D_{XY} estimated from Illumina data did not show high divergence (0.78–3.01) among the population pairs around the SCS (including populations in the "n-SCS" and "s-SCS", Figure S6).

3.3 | Haplotype grouping and geographical distribution

The haplotype networks based on all six Sanger-sequenced genes robustly showed the major break between Asia and Australasia. Particularly, within each of the five defined subgroups, the populations compose the same cluster of closely related haplotypes in all six genes. However, we observed in almost all genes that two or more subgroups shared the same cluster of haplotypes. In the A189 gene, the "Indo-Malayan", "s-SCS" and "Australasia" populations compose distinct haplotypes (Figure 3a). Within "Indo-Malayan", haplotypes in "Gulf of Bengal" are different from those in "n-SCS". In gene A414, the whole "Indo-Malayan" group shared haplotypes, with the two populations on the west coast of the Malay Peninsula (La-un and Ngao) having distinctive haplotypes. A cluster of haplotypes also occurred strongly in Chai-ya and to a lesser extent in other populations of the South China Sea (Figure 3b). In the A440 gene, the "Indo-Malayan" and "Pan-Australasia" populations show distinct haplotypes (Figure 3c). For the A245 gene, each of the "s-SCS", "n-SCS", "Gulf of Bengal" and "Australasia" subgroup show distinct haplotypes (Figure 3d). In the C058 gene, "s-SCS" share haplotypes with the "Bali" subgroup, while "Australasia" and "Indo-Malayan" (excepting Bali) show distinct haplotypes (Figure 3e). In the A383 gene, the "s-SCS", "Australasia" and "Bali" populations shared a cluster of haplotypes, while the "n-SCS" and "Gulf of Bengal" populations had divergent haplotypes (Figure 3f).

As the six Sanger-sequenced genes showed contrasting patterns, we constructed haplotypes from the Illumina sequences. Haplotypes were inferred based on the linkage information of short reads, with the 93 genes split into segments (see Methods). We retained the 84 segments with lengths longer than 300 bp for the following analyses (Table S2). Forty-three of the 84 segments showed no divergent haplotype groups, with their haplotype networks showing a loop- or star-like topology. The remaining 41 segments showed 2–5 divergent clusters. (1) Twelve segments split into three clusters, with one distributed in the "Indo-Malayan" populations, the second in "s-SCS" and the last in "Australasia" (Figure 4a); (2) eight segments split into two clusters, with one in Asia (including the "Indo-Malayan" and "s-SCS") and the other in "Australasia" (Figure 4b); (3) six segments split into two clusters: "Indo-Malayan" and "Pan-Australasia" (Figure 4c); (4) six segments fell into five divergent haplotype groups, with each of the five second-level group composites a cluster (Figure 4d); (5) five segments split into three clusters: "n-SCS and Gulf of Bengal", "s-SCS and Bali", and "Australasia" (Figure 4e); and finally, (6) four segments split into three clusters: "n-SCS", "s-SCS, Gulf of Bengal and Bali", and "Australasia" (Figure 4f).

In short, consistent with the pattern of population clustering revealed above, the divergence of haplotypes was most frequently found between the two groups of "Indo-Malayan" and "Pan-Australasia", and the divergence of haplotypes was also found between subgroups at lower frequencies. Within each subgroup, the populations always shared same haplotypes. The sharing of haplotypes between subgroups occurred in different genes with different combinations of subgroups.

3.4 | Geographical barrier identification and test of isolation by distance

By calculating Monmonier's maximum difference using the program BARRIER, we inferred four strong geographic barriers. The robustness of each barrier was assessed by bootstrapping over 100 matrices of F_{ST}, with each matrix calculated from 30 genes randomly sampled from the 93 sequenced genes. The first barrier, supported by the 99 F_{ST} matrix, aligns with the Malay Peninsula, isolating La-un and Nago from Chai-ya (Figure 5a). The second barrier, with the support of 85 matrices, lies in the Indonesian archipelago, isolated Bali from Kuching (Figure 5a). Both of the two barriers are part of the Sundaland barrier. The third barrier lies in the Wallacea region, supported with 93, 75, and 75 matrices (Figure 5a). This barrier isolated the populations in Australasia from those in Southeast Asia. The fourth barrier, which is supported by 95, 95, and 59 matrices, lies between the northern South China Sea and southern South China Sea (Figure 5a).

The Mantel test revealed a significant correlation ($r = 0.518$, p-value $< .01$) between geographical distance and genetic differentiation of Sanger F_{ST} estimations (Figure 5b). The same test using Illumina data also showed a significant correlation ($r = 0.485$, p-value $< .01$, Figure S7). The Mantel tests within the "Pan-Australasia" group ($r = 0.560$, p-value $< .01$, Figure S8) and "Indo-Malayan" group ($r = 0.698$, p-value $< .01$, Figure S9) showed even stronger correlations. This indicated isolation by distance has contributed to the population differentiation. However, the observed F_{ST} values of

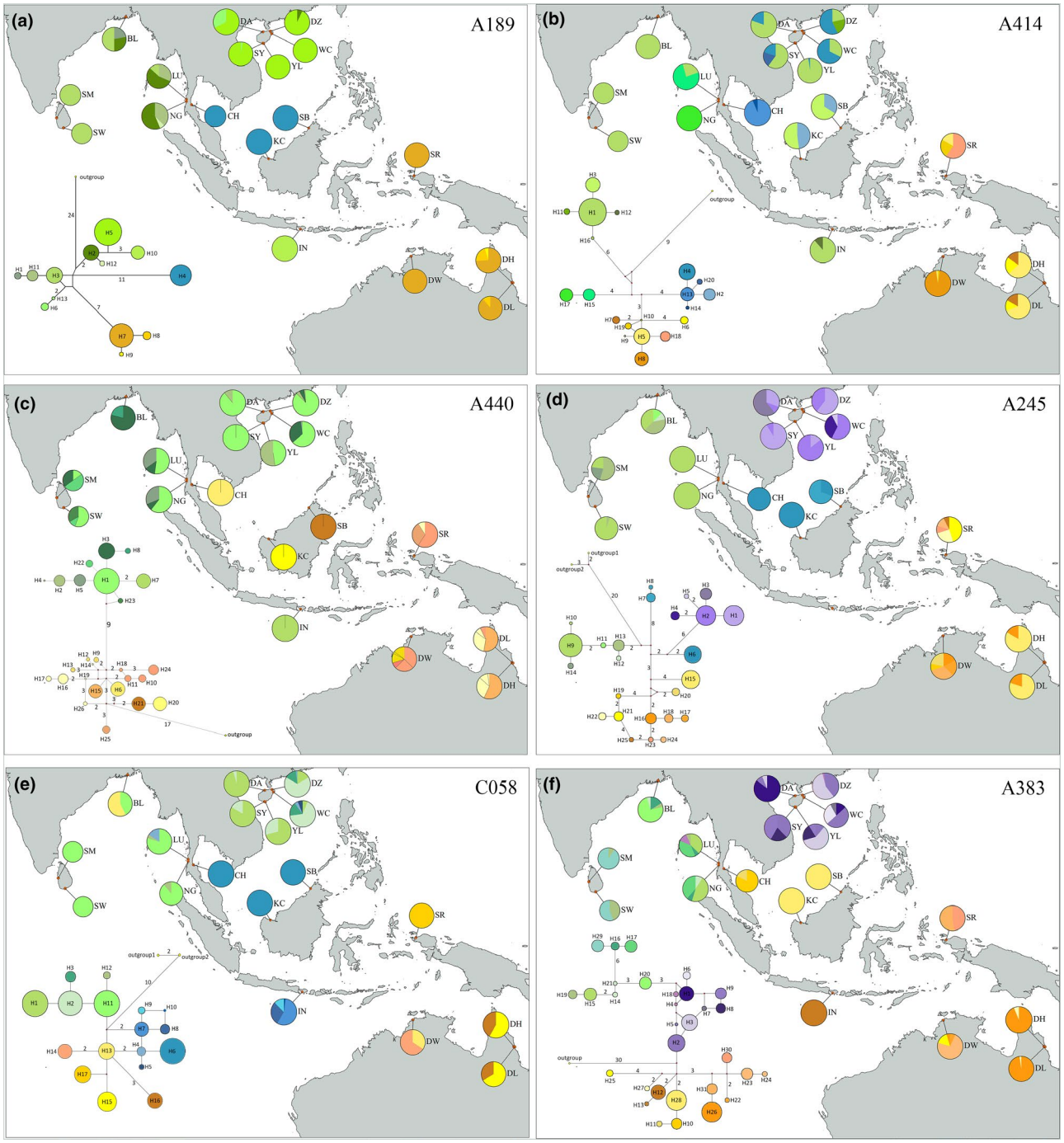

FIGURE 3 Geographical distribution patterns of the haplotypes inferred in the 6 Sanger-sequenced genes. The corresponding haplotype networks are drawn in the lower left corners of the maps. The colours corresponded to the haplotypes. Each haplotype is represented by a unique colour and closely related haplotypes are represented by similar colours. In the haplotype network, the circle size is approximately proportional to the number of individuals of each haplotype. The number beside the lines indicates the mutation steps. The representative gene ID of each pattern is written to its upper right

population pairs within each subgroup are much smaller than the expected ones under the IBD assumption (Figure 5b). Meanwhile, the observed F_{ST} values are larger than the expected ones in the population pairs of s-SCS and n-SCS as well as s-SCS and the Indian Ocean (Figure 5b). These deviations from the IBD expectations complement the pattern of population grouping revealed above.

3.5 | Bottleneck event revealed by simulations

We employed the approximate Bayesian computation (ABC) method to test 12 possible models (Figure 6a). By simulations, model 8 acquired the highest posterior probability, which assumed that the "s-SCS" populations shared a common ancestor with "Australasia",

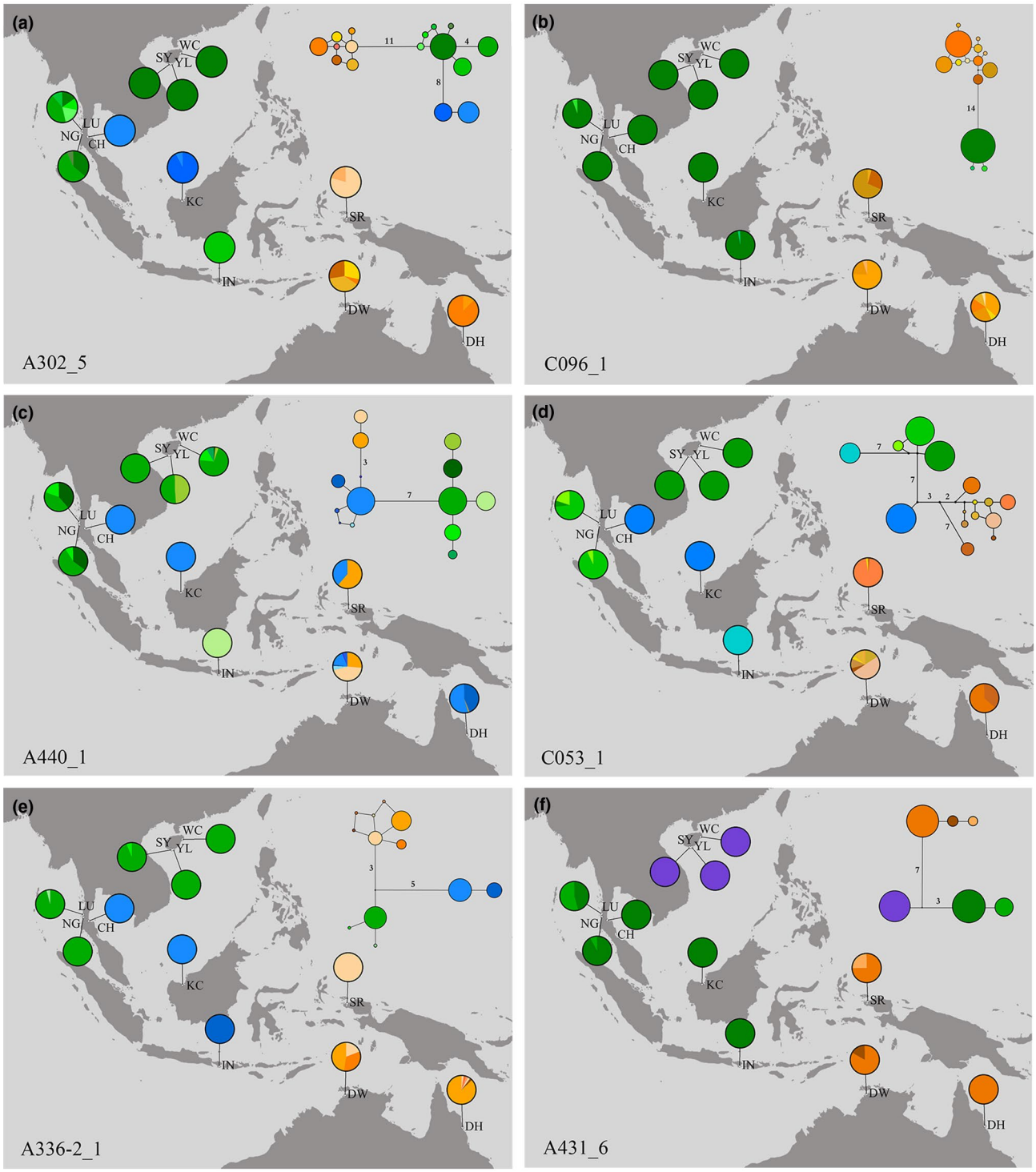

FIGURE 4 Six different geographical distribution patterns of the haplotypes inferred from the 41 Illumina-sequenced genes. The corresponding haplotype network is drawn in the upper right corner of each map. The colours corresponded to the haplotypes. Each haplotype is represented by a unique colour and closely related haplotypes are represented by similar colours. In the haplotype network, the circle size is approximately proportional to the number of individuals of each haplotype. The small black nodes on the lines are the median vectors, indicating the hypothesized (often ancestral) sequences required to connect the existing sequences within the network with maximum parsimony. The number beside the lines indicates the mutation steps. The representative gene segment ID of each pattern is written to its lower left

then "s-SCS" diverged with "Australasia", accompanied by a severe bottleneck, and recently expanded to its current population size (Figure 6a). Migrations between the "Indo-Malayan" and "s-SCS" or between "Australasia" and "s-SCS" have occurred in recent times. This model choice is robust, with a posterior probability larger than 0.6 in all three repeated computations (Table 3).

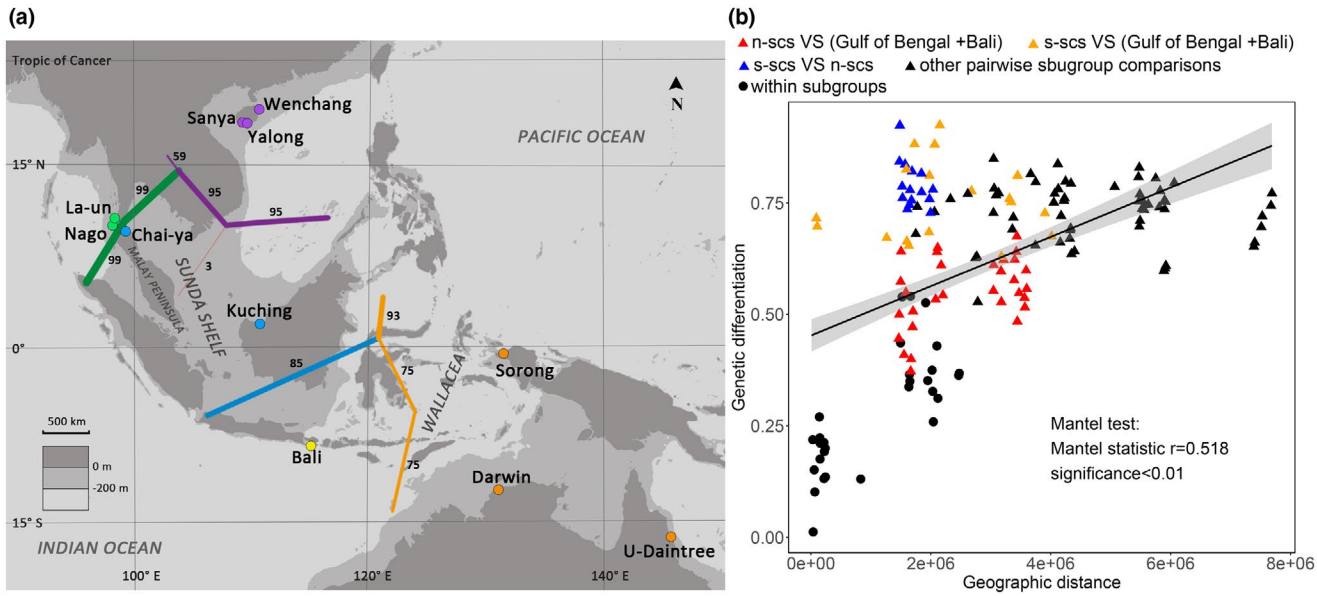

FIGURE 5 Geographical factors underlying the genetic structure of *Aegiceras corniculatum* revealed by BARRIER inference and Mantel test. (a) Results of the barrier analysis (Manni et al., 2004) based on Illumina-sequencing data, showing the spatial separation of *Ae. corniculatum* populations. The detected barriers (thick coloured lines) separate 11 populations into five groups. Green, blue, orange and purple lines correspond to the first, second, third and fourth barriers. The thickness of a coloured line indicates the number of F_{ST} matrices (black number adjacent to the line) that support the corresponding barrier. (b) Mantel test based on the F_{ST} matrices of six Sanger-sequenced genes. Different types of population pairs were indicated with different marks and colours

Under the optimal demographic history model, we estimated the posterior distribution of the demographic parameters. The "Indo-Malayan" lineage and the ancestor of the "Australasia" and "s-SCS" (the "Pan-Australasia" group) diverged approximately 2.7 million years ago (Ma) (95% confidence interval, i.e., CI: 2.6–3.0). Next, the "s-SCS" lineage diverged from the "Australasia" lineage approximately 1.5 million years ago (95% CI: 1.2–1.9). N_0 was estimated as 1,916. Accordingly, the population size of the ancestral "s-SCS" lineage was estimated to have reduced from 10,538 to 824 (5.5 N_0 to 0.43 N_0) in the bottleneck event. Since approximately 0.13 million years ago (95% CI: 0.1–0.2), the N_e of the "s-SCS" lineage has increased gradually to 1,917 (95% CI: 1812–1986). The N_e values of the "Indo-Malayan" and "Australasia" lineages were relatively constant, at 9,580 and 10,538, respectively. Gene flow was asymmetric, that the values are 0.258 per generation (95% CI: 0.118–0.688) from the "Indo-Malayan" to the "s-SCS" populations and 0.007 (95% CI: 0.002–0.021) in the reciprocal direction. Similarly, the gene flow was 0.403 (95% CI: 0.216–0.775) per generation from the "Australasia" to the "s-SCS" populations, and the reciprocal flow was 0.005 (95% CI: 0–0.075) per generation (Table 4).

The method of Stairway Plot 2 (Liu & Fu, 2020) was also used to obtain an estimation of the dynamic history of N_e. Consistent with the estimation of ABC simulations, a sharp decrease of N_e from c. 6,000 to c. 1,100 is observed in lineage 1 (s-SCS) (Figure 6b). Notably, the N_e reduction occurred about 6,000 years ago, if we assume the generation time is 20 years. In comparison, the N_e values of lineage 2 and lineage 3 are relatively stable in the past. Although a trend of slow decrease is observed in lineage 2, the N_e has remained over 5,000 (Figure 6c). The N_e of lineage 3 has also remained constant over 10,000 in the past 100,000 years (Figure 6d). Although a reduction of N_e occurred c. 200,000–100,000 years ago in Lineage 3, the N_e remained as large as c. 10,000 even after the reduction (Figure 6d). In short, both the ABC simulations and Stairway Plot 2 clearly reveal the severe bottleneck event in the southern South China Sea, while much more constant population sizes in the other lineages. Although the time scales of the ABC method and Stairway Plot differ, probably due to the different sensitivities in parameter estimation of the two methods, the patterns of population size change agree well.

4 | DISCUSSION

4.1 | Geographical barriers played a fundamental role in shaping genetic structuring of coastal plant species

In addition to open oceans that are too wide for propagules to pass through, land barriers and ocean currents are commonly found to hinder the dispersal of coastal plant species that disperse propagules via seawater (Kadereit et al., 2005; Yang et al., 2012). Mangrove species, which are the most typical coastal plants, strictly inhabit the intertidal zones and disperse via buoyant propagules such as fruits, seeds, and hypocotyls. The propagules of some species can float at sea for months before reaching a new intertidal habitat (Tomlinson, 2016). However, the phylogeographical patterns of mangrove

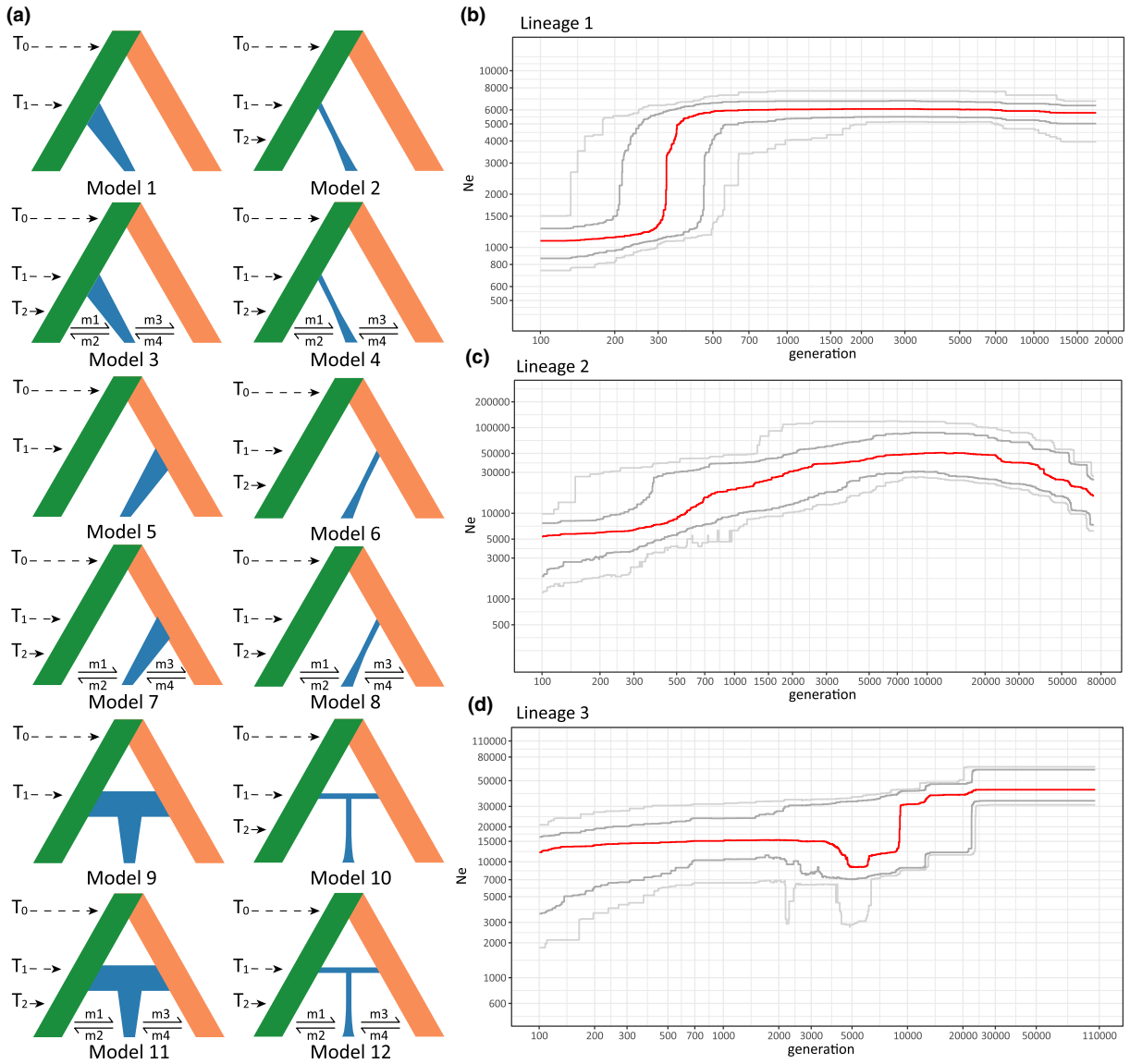

FIGURE 6 Demographic history of the populations of *Aegiceras corniculatum*. (a) Twelve models simulating the demographic history. Blue indicates Lineage 1, which includes Kuching and Chai-ya. Orange indicates Lineage 2, which includes U-Daintree, Darwin, and Sorong. Green indicates Lineage 3, which includes Sanya, Wenchang, Yalong, La-un, Ngao and Bali. The double-sided arrow indicates migration. T_0–T_2 indicate the time points of historic events and m_1–m_4 indicate gene flows. (b–d) Stairway plots for Lineage 1 (b), Lineage 2 (c) and Lineage 3 (d). The red line indicates the median of N_e estimation based on 200 inferences, and the grey and light grey lines indicate 75% and 95% confidence intervals

species have been fundamentally shaped by land barriers and ocean currents, such as the Central American Isthmus to *Rhizophora mangle* or *R. racemosa* (Takayama et al., 2013) and the ocean currents at the northeastern extremity of South America to *R. mangle*, *Avicennia germinans* or *Av. schaueriana* (Mori et al., 2015; Pil et al., 2011).

The Indo-West Pacific region, particularly Southeast Asia, is the hotspot of mangrove species diversity (Duke, 2017), thus the majority of the studies discussing phylogeography of mangrove species concentrated on this region. The Malay Peninsula (or the Sundaland when sea level was low) was identified to be the most dominant land barrier for mangrove species. Genetic discontinuity between the Indian ocean and Pacific Ocean sides of Sundaland has been observed in *R. apiculata* (Guo et al., 2016), *R. mucronata* (Yan et al., 2016), *Av. marina* (Wang et al., 2021), *Sonneratia alba* (Yang et al., 2017), *S. caseolaris* (Yang et al., 2016), *Ceriops tagal* (Huang et al., 2012), *C. decandra* (Huang et al., 2008), *Xylocarpus* species (Guo, Ng, et al., 2018), *Lumnitzera racemosa* (Li et al., 2016), *Bruguiera gymnorhiza* (Minobe et al., 2010; Urashi et al., 2013), *Excoecaria agallocha* (Guo, Ng, et al., 2018), *Heritiera littoralis* (Banerjee et al., 2020), *Scaevola taccada* (Banerjee et al., 2021) and *Acanthus ilicifolus* (Guo et al., 2020). In this study, the Malay Peninsula was again identified to isolate populations of *Ae. corniculatum*. The isolation of Sundaland corresponds to the population differentiation between the subgroup "Gulf of Bengal" and "n-SCS", as well as "Bali" and "n-SCS". Despite its dominant role in mangrove species, the barrier effect of the Malay Peninsula receded largely in some coastal plants that

inhabit more inland, such as *Canavalia rosea* (He et al., 2021) and *Pluchea indica* (Lin et al., 2020).

Genetic discontinuities in a lot of mangrove species also occur in the Wallacea region where the Indonesian-through flow functions as a major barrier hindering the dispersal of propagules. This barrier generates a population structure that populations in Southeast Asia are divergent from those in Australasia. Such pattern has been observed in the species of *R. apiculata* (Guo et al., 2016), *R. stylosa* (Yan et al., 2016), *S. alba* (Yang et al., 2017), *S. caseolaris* (Yang et al., 2016), *Av. marina* (Wang et al., 2021), *C. tagal* (Huang et al., 2008, 2012), *C. decandra* (Huang et al., 2008), *X. granatum* (Guo, Guo, et al., 2018), and *L. racemosa* (Li et al., 2016). This water barrier appears less dominant that populations of several species are not isolated, e.g. *Acanthus ilicifolus* (Guo et al., 2020), *H. littoralis* (Banerjee et al., 2020), *Scaevola taccada* (Banerjee et al., 2021), and *X. mucronata* (Guo, Guo, et al., 2018). The difference in the ability to disperse across the sea currents may underlie the different population structures, even in congeneric species like *X. granatum* and *X. mucronata* (Guo, Guo, et al., 2018). The populations of *Ae. corniculatum* showed a slight genetic break aligning with the Wallacea barrier. The hypocotyl of *Ae. corniculatum* is reported to have a relatively strong long-distance dispersal ability (Clarke et al., 2001).

IBD might have played a role in differentiating populations of coastal plants. Our mantel test revealed a significant positive correlation between genetic distance and geographic distance. For example, the long distance between "Bali" and "Gulf of Bengal" is probably the factor underlying their slight genetic differentiation. Despite the dispersal ability, it is understandable to observe the IBD effect in *Ae. corniculatum* across the very large geographical scale of its distribution range.

The patterns discussed above are generally consistent with previous knowledge. However, the striking genetic break between "s-SCS" and "n-SCS" is quite intriguing, some unaddressed factors should have been in function. We address this issue in the next section.

TABLE 3 Posterior probabilities of models using approximate Bayesian computation

	Repeat 1	Repeat 2	Repeat 3
Model 1	0.0000	0.0000	0.0015
Model 2	0.0000	0.0000	0.0018
Model 3	0.0002	0.0000	0.0073
Model 4	0.0019	0.0004	0.0114
Model 5	0.0011	0.1878	0.1189
Model 6	0.2851	0.0449	0.0507
Model 7	0.0320	0.0290	0.0394
Model 8	0.6332	0.7109	0.6803
Model 9	0.0000	0.0009	0.0048
Model 10	0.0048	0.0020	0.0079
Model 11	0.0028	0.0017	0.0141
Model 12	0.0389	0.0225	0.0619

4.2 | Sea-level-change-driven bottleneck enhanced population subdivision in the southern South China Sea

The genetic discontinuity between the "s-SCS" and "n-SCS" actually is not unique in *Ae. corniculatum*. The studies of mangrove species *E. agallocha* (Guo, Ng, et al., 2018) and *H. littoralis* (Banerjee et al., 2020) have also shown similar genetic discontinuities. The previous studies suggested that these genetic discontinuities are attributed to the lack of suitable ocean currents to disperse fruits during the ripening season in the South China Sea (Banerjee et al., 2020; Guo, Ng, et al., 2018). We argue that at least two observations in *Ae. corniculatum* are not compatible with the previous explanation. First, the differentiation between "n-SCS" and "Gulf of Bengal" is much lower than between "s-SCS" and "Gulf of Bengal". How could "n-SCS" populations exchange genes with "Gulf of Bengal" populations without bridging by "s-SCS" populations? Second, the differentiation between "s-SCS" and "n-SCS" is comparable to between "s-SCS" and "Gulf of Bengal",

TABLE 4 Estimates of the principal demographic parameters for the best supported ABC models

Parameters	Ne	T_0 (myr)	T_1 (myr)	T_2 (myr)	m_1	m_2	m_3	m_4	Bottleneck
Mode	1917	2.711	1.493	0.127	0.258	0.007	0.005	0.403	0.427
95% CI (lower)†	1812	2.585	1.236	0.104	0.118	0.002	0	0.216	0.18
95% CI (upper)	1986	3.014	1.858	0.206	0.688	0.021	0.075	0.775	0.485

Note: Ne represents the number of diploid individuals in the population.

T_0 represents the time the "Indo-Malayan" lineage and the ancestor of the "Australasia" and "s-SCS" lineages diverged. The unit of time is million years.

T_1 represents the time the "s-SCS" lineage diverged from the "Australasia" lineage. The unit of time is million years.

T_2 represents the time the N_e of the "s-SCS" lineage increased. The unit of time is million years.

m_1, m_2, m_3, and m_4 represent the gene flow from the "Indo-Malayan" to the "s-SCS" populations, from the "s-SCS" to the "Indo-Malayan" populations, from the "s-SCS" to the "Australasia" populations, and from the "Australasia" to the "s-SCS" populations, respectively.

Bottleneck represents the proportion of N_e reduced.

†95% CI indicates the 95% confidence intervals.

much higher than that between "s-SCS" and "Australasia". It's not feasible to assume that the influence of ocean currents in the SCS is even stronger than that of the Indonesian-through flow, to a level comparable with the land barrier of the Malay Peninsula. Hence, the break between the "s-SCS" and "n-SCS" populations of *Ae. corniculatum* cannot be simply attributed to the influence of ocean currents.

We hypothesized that bottleneck events could promote population subdivision by augmenting population differentiation. The "s-SCS" cluster was found to have undergone a bottleneck event. Our ABC simulations provided strong support that the "s-SCS" population originated from the "Australasia" cluster, with the split occurring at ~1.5 Ma. The close relationship between "s-SCS" and "Australasia" was also evidenced directly by STRUCTURE and PCA clustering, and low F_{ST} values. During the split, the "s-SCS" population was reduced to a population size of ~824, from 10538 of the common ancestral population. This bottleneck is also revealed in our Stairway Plot. The drastic reduction of genetic diversity in the populations Chai-ya and Kuching also evidenced the bottleneck event. The average π values in the populations Chai-ya and Kuching are only 14.3%–24.4% of those in the populations of "Australasia" subgroup and the average θ values are only 11.2%–25.6% (Table 2). In other words, at least 75%–90% of the ancestral polymorphisms were lost during the bottleneck event, which is consistent with the ~92% reduction in effective population size estimated by ABC modelling.

Although the time estimation using ABC computation may not be very accurate, it roughly dated the origination of the "s-SCS" cluster in the middle of Pleistocene, when glacial periods alternated with interglacial periods repeatedly. During the glacial periods (Miller et al., 2005; Voris, 2000), most Southeast Asia populations should have been wiped out. The refugial populations might have contracted to the margins of the Sundaland with a range from Wallacea to North Australia. As sea level rose in the interglacial periods, a subset of the refugia population expanded to the current southern South China Sea range as the coastline advanced (Cannon et al., 2009). Such a process could have repeated multiple times. However, the genetic data obtained today are powerless to distinguish them because the ancient genetic patterns have been reshaped by more recent events.

During the bottleneck processes, intensified genetic drift and relaxed purifying selection due to reduced population size should have contributed to the loss of ancestral polymorphisms and fixation of new mutations. The observation of haplotypes unique to the "s-SCS" cluster in many genes is consistent with this interpretation. This mechanism consequently generated the current deep genetic differentiation between "s-SCS" and "n-SCS". Despite the bottleneck effect, the gene flow between "s-SCS" and "n-SCS" seems not completely blocked, evidenced by the occurrence of "n-SCS" haplotypes with relatively high frequency in "s-SCS" populations. Our ABC modeling also supported the existence of such gene flow. In contrast, gene flow in the reciprocal direction is much lower, indicated by that "s-SCS" haplotypes were rarely observed in "n-SCS" populations. This asymmetric gene flow may be attributed to the different adaptabilities of propagules. The propagules migrated from the colder marginal regions (e.g., n-SCS) may be relatively easy to colonize in the warm equatorial region (s-SCS) while propagules migrated in the reverse direction may be less successful to cope with the cold weather.

As mentioned before, the substantial genetic break between "s-SCS" and "n-SCS" has also been observed in *E. agallocha* (Guo, Ng, et al., 2018) and *H. littoralis* (Banerjee et al., 2020), which may also be attributed to the mechanism we described above. However, the mismatch distribution analyses presented in the original papers provided no support for a sudden expansion model (Banerjee et al., 2020; Guo, Ng, et al., 2018). Notably, obvious differentiation has been observed between the populations sampled from Northeastern Borneo and surrounding populations in *S. alba* (Yang et al., 2017) and *Av. marina* (Wang et al., 2021). Such population structures in the smaller geographical ranges are highly likely generated by a bottleneck process. Further studies may test this hypothesis in these species. In contrast, the populations of some mangrove species, whose distribution range covers both the northern and southern parts of the South China Sea, are found to be genetically continuous with confidential data. Such species include but are not limited to *R. apiculata* (Guo et al., 2016), *R. stylosa* (Yan et al., 2016), *C. decandra* (Huang et al., 2012), *B. gymnorhiza* (Urashi et al., 2013), and *L. racemose* (Li et al., 2016). The genetic homogeneity of northern and southern South China Sea in these species may be attributed to two possible mechanisms. Firstly, the extremely low level of genetic diversity indicates the populations of both regions may be sourced from a single refugium that survived the sea-level fluctuations (Guo, Li, et al., 2018). Secondly, the recent gene flow may have eliminated historic genetic differentiation due to the strong dispersal ability of these species (Clarke et al., 2001; Guo et al., 2016; Urashi et al., 2013). Different species may have been impacted by the historic sea-level fluctuation to different extents, resulting in different current genetic patterns. Compared to those genetic structures attributed to geographical barriers, the population structure generated by bottleneck events appears to be rarer and more unpredictable.

4.3 | Demographic size dynamics such as bottleneck may be a general mechanism to shape the genetic structure of coastal plants

Consistent with our hypothesis, we observed that the bottleneck event caused by past sea-level changes have promoted population subdivision in *Ae. corniculatum*, resulting in the genetic break between populations in the southern and northern South China Sea. This mechanism is not probably unique to *Ae. corniculatum*, but general to other species. The intraspecific genetic diversity of *Senecio rodriguezii* was found to be highly structured in that cpDNA haplotypes were not shared between the Mediterranean islands and a high proportion of haplotypes were restricted to small geographical areas within the islands (Molins et al., 2009). The population history of this species was supposed to have been dominated by both expansion and contraction events in the Quaternary sea-level changes. The

three major lineages of *Nigella arvensis* in the Aegean Archipelago were found to evolve from multiple fragmentation events of a widespread ancestral stock, in which genetic drift appears to have played a significant role (Bittkau & Comes, 2005).

The mechanism of bottleneck events promoting population subdivision is highly likely applicable to coastal plants, which are common to have buoyant propagules, even in species growing on coastal dunes which are rarely inundated by seawater (Kadereit et al., 2005; Yang et al., 2012). Due to the nature of dispersing via seawater, genetic discontinuities in coastal plants were usually correlated with geographical barriers of land masses and ocean currents. It has known that biological properties of a species, such as breeding system, dispersal ability, and life history, would have an influence on how the geographic forces shape genetic variation within its distribution range (Nybom & Bartish, 2000; Wee et al., 2020; Westberg & Kadereit, 2009). We showed that the high dynamics of the habitats of coast plants may introduce additional complexity to their phylogeography.

The demographic histories of some coastal plants in the Indo-West Pacific region have been investigated. The effective population size (N_e) of *R. apiculata* populations in the Malacca Strait (Guo et al., 2016) and *L. racemosa* populations in the Malacca Strait and Hainan island were found to have been drastically reduced (Li et al., 2016). In contrast, the *S. alba* populations in the Malacca strait have larger N_e than the surrounding populations, due to population admixture (Yang et al., 2017). The mismatch distribution analysis and neutrality tests revealed some signals of population expansion in *Acanthus ilicifolius* (Guo et al., 2020) while the BOTTLENECK analysis revealed no evidence of genetic bottleneck in *Canavalia rosea* (He et al., 2021). Interestingly, the possible correlation between genetic structure and historic demographic size change was not explored in these studies. Even if the mechanism we proposed before is general in the natural world, a reliable investigation into the bottleneck event must precede correlating it to any observed genetic break.

Lastly, attention to the demographic size change of a species is of particular importance for conservation. A large population is usually the fundament for plants to provide ecological services. The ecological importance of mangrove species has never been overly emphasized. Investigating their historic effective population sizes is an efficient approach to retrospect their past and prospect their future response to the current global change (Guo, Li, et al., 2018). The *Ae. corniculatum* populations in the southern South China Sea call for conservation priority due to the reduced genetic diversity.

ACKNOWLEDGEMENTS

This study was supported by the Guangdong Basic and Applied Basic Research Foundation (grant number 2021A1515011160),the National Natural Science Foundation of China (grant numbers 31830005 and 31900200); the National Key Research and Development Plan (2017FY100705); the China Postdoctoral Science Foundation (grant no. 2019M663212); and the Chang Hungta Science Foundation of Sun Yat-Sen University.

AUTHOR CONTRIBUTIONS

Zixiao Guo and Suhua Shi conceived the study. Suhua Shi, Lu Fang, Cairong Zhong, and Norman C. Duke collected the samples. Rufan Zhang, Zixiao Guo, and Lu Fang analysed the data. Zixiao Guo, Rufan Zhang and Suhua Shi wrote the manuscript. All authors read and approved the manuscript.

CONFLICT OF INTEREST

The authors declare no conflict of interest.

OPEN RESEARCH BADGES

This article has earned an Open Data Badge for making publicly available the digitally-shareable data necessary to reproduce the reported results. The data were deposited to Genome Sequence Archive in National Genomics Data Center (accession number CRA004437).

DATA AVAILABILITY STATEMENT

GenBank accession numbers of reference sequences for the genes are KF745073, KF745075- KF745085, KF745087- KF745088, KF745090, KF745092, KF745095- KF745097, KF745099- KF745106, KF745108- KF745111 KF745113- KF745125, KF745127- KF745130, KF745132- KF745139, KF958338, KF958340, KF958343- KF958345, and KF977861-KF977866 (the detailed information could be found in the supplementary Table S2 of He et al., 2019, https://doi.org/10.1093/nsr/nwy078). The raw reads of Illumina sequencing data have been deposited in the Genome Sequence Archive at the National Genomics Data Center (accession no. CRA004437). The Sanger sequences of population individuals have been deposited to NCBI (accession no.PRJNA739874).

ORCID

Zixiao Guo https://orcid.org/0000-0003-4820-4056

REFERENCES

Allen, G. C., Flores-Vergara, M. A., Krasynanski, S., Kumar, S., & Thompson, W. F. (2006). A modified protocol for rapid DNA isolation from plant tissues using cetyltrimethylammonium bromide. *Nature Protocols*, *1*(5), 2320–2325. http://dx.doi.org/10.1038/nprot.2006.384

Bandelt, H. J., Forster, P., & Röhl, A. (1999). Median-joining networks for inferring intraspecific phylogenies. *Molecular Biology and Evolution*, *16*(1), 37–48. https://doi.org/10.1093/oxfordjournals.molbev.a026036

Banerjee, A. K., Guo, W., Qiao, S., Li, W., Xing, F., Lin, Y., ... & Huang, Y. (2020). Land masses and oceanic currents drive population structure of *Heritiera littoralis*, a widespread mangrove in the Indo-West Pacific. *Ecology and Evolution*, *10*(14), 7349–7363.

Banerjee, A. K., Wu, H., Guo, W., Ng, W. L., Li, W., Ma, Y., ... & Huang, Y. (2021). Deciphering the global phylogeography of a coastal shrub (*Scaevola taccada*) reveals the influence of multiple forces on contemporary population structure. *Journal of Systematics and Evolution*, https://doi.org/10.1111/jse.12746

Barbier, E. B., Hacker, S. D., Kennedy, C., Koch, E. W., Stier, A. C., & Silliman, R. (2011). The value of estuarine and coastal ecosystem services. *Ecological Monographs*, *81*(2), 169–193. https://doi.org/10.1890/10-1510.1

Bay, L. K., Caley, M. J., & Crozier, R. H. (2008). Meta-population structure in a coral reef fish demonstrated by genetic data on patterns of migration, extinction and re-colonisation. *BMC Evolutionary Biology*, *8*(1), 1–17. https://doi.org/10.1186/1471-2148-8-248

Beaumont, M. A., Zhang, W., & Balding, D. J. (2002). Approximate Bayesian computation in population genetics. *Genetics*, *162*(4), 2025–2035. https://doi.org/10.1093/genetics/162.4.2025

Bittkau, C., & Comes, H. (2005). Evolutionary processes in a continental island system: Molecular phylogeography of the Aegean *Nigella arvensis alliance* (Ranunculaceae) inferred from chloroplast DNA. *Molecular Ecology*, *14*, 4065–4083. https://doi.org/10.1111/j.1365-294X.2005.02725.x

Cannon, C. H., Morley, R. J., & Bush, A. B. G. (2009). The current refugial rainforests of Sundaland are unrepresentative of their biogeographic past and highly vulnerable to disturbance. *Proceedings of the National Academy of Sciences - PNAS*, *106*(27), 11188–11193. https://doi.org/10.1073/pnas.0809865106

Clarke, P. J., Kerrigan, R. A., & Westphal, C. J. (2001). Dispersal potential and early growth in 14 tropical mangroves: Do early life history traits correlate with patterns of adult distribution? *Journal of Ecology*, *89*(4), 648–659. https://doi.org/10.1046/j.0022-0477.2001.00584.x

Csilléry, K., François, O., & Blum, M. G. B. (2012). Abc: An R package for approximate Bayesian computation (ABC). *Methods in Ecology and Evolution*, *3*(3), 475–479. https://doi.org/10.1111/j.2041-210X.2011.00179.x

Demastes, J. W., Hafner, D. J., Hafner, M. S., Light, J. E., & Spradling, T. A. (2019). Loss of genetic diversity, recovery and allele surfing in a colonizing parasite, Geomydoecus Aurei. *Molecular Ecology*, *28*(4), 703–720. https://doi.org/10.1111/mec.14997

Deng, S., Huang, Y., He, H., Tan, F., Ni, X., Jayatissa, L. P., Hettiarachi, S., & Shi, S. (2009). Genetic diversity of Aegiceras corniculatum (Myrsinaceae) revealed by amplified fragment length polymorphism (AFLP). *Aquatic Botany*, *90*(4), 275–281. http://dx.doi.org/10.1016/j.aquabot.2008.11.002

Duke, N. C. (2014). *'World Mangrove iD: expert information at your fingertips' Version 1.1 for Android*. MangroveWatch Ltd. https://doi.org/10.13140/2.1.1533.1842

Duke, N. C. (2017). Mangrove floristics and biogeography revisited: further deductions from biodiversity hot spots, ancestral discontinuities, and common evolutionary processes. *Mangrove Ecosystems: A Global Biogeographic Perspective Structure, Function, and Services*. Switzerland: Springer. https://doi.org/10.1007/978-3-319-62206-4

Evanno, G., Regnaut, S., & Goudet, J. (2005). Detecting the number of clusters of individuals using the software STRUCTURE: A simulation study. *Molecular Ecology*, *14*(8), 2611–2620. https://doi.org/10.1111/j.1365-294X.2005.02553.x

Falush, D., Stephens, M., & Pritchard, J. K. (2003). Inference of population structure using multilocus genotype data: Linked loci and correlated allele frequencies. *Genetics*, *164*(4), 1567–1587. https://doi.org/10.1111/j.1471-8286.2007.01758.x

Foufopoulos, J., Kilpatrick, A. M., & Ives, A. R. (2011). Climate change and elevated extinction rates of reptiles from Mediterranean islands. *American Naturalist*, *177*(1), 119–129. https://doi.org/10.1086/657624

Ge X. - J., Hung K. - H., Ko Y. - Z., Hsu T. - W., Gong X., Chiang T. - Y., & Chiang Y. - C. (2015). Genetic Divergence and Biogeographical Patterns in Amentotaxus argotaenia Species Complex. *Plant Molecular Biology Reporter*, *33*(2), 264–280. http://dx.doi.org/10.1007/s11105-014-0742-0

Ge, X. J., & Sun, M. (1999). Reproductive biology and genetic diversity of a cryptoviviparous mangrove *Aegiceras corniculatum* (Myrsinaceae) using allozyme and intersimple sequence repeat (ISSR) analysis. *Molecular Ecology*, *8*(12), 2061–2069. https://doi.org/10.1046/j.1365-294x.1999.00821.x

Guo, W., Banerjee, A. K., Ng, W. L., Yuan, Y., Li, W., & Huang, Y. (2020). Chloroplast DNA phylogeography of the Holly mangrove *Acanthus ilicifolius* in the Indo-West Pacific. *Hydrobiologia*, *847*(17), 3591–3608. https://doi.org/10.1007/s10750-020-04372-1

Guo, W., Ng, W. L., Wu, H., Li, W., Zhang, L., Qiao, S., Yang, X., Shi, X., & Huang, Y. (2018). Chloroplast phylogeography of a widely distributed mangrove species, *Excoecaria agallocha*, in the Indo-West Pacific region. *Hydrobiologia*, *807*(1), 333–347. https://doi.org/10.1007/s10750-017-3409-7

Guo, Z., Guo, W., Wu, H., Fang, X., Ng, W. L., Shi, X., … & Huang, Y. (2018). Differing phylogeographic patterns within the Indo-West Pacific mangrove genus Xylocarpus (Meliaceae). *Journal of Biogeography*, *45*(3), 676–689. https://doi.org/10.1111/jbi.13151

Guo, Z., Huang, Y., Chen, Y., Duke, N. C., Zhong, C., & Shi, S. (2016). Genetic discontinuities in a dominant mangrove Rhizophora apiculata (Rhizophoraceae) in the Indo-Malesian region. *Journal of Biogeography*, *43*, 1856–1868. https://doi.org/10.1111/jbi.12770

Guo, Z., Li, X., He, Z., Yang, Y., Wang, W., Zhong, C., Greenberg, A. J., Wu, C.-I., Duke, N. C., & Shi, S. (2018). Extremely low genetic diversity across mangrove taxa reflects past sea level changes and hints at poor future responses. *Global Change Biology*, *24*(4), 1741–1748. https://doi.org/10.1111/gcb.13968

Haanes, H., Røed, K. H., Flagstad, Ø., & Rosef, O. (2010). Genetic structure in an expanding cervid population after population reduction. *Conservation Genetics*, *11*(1), 11–20. https://doi.org/10.1007/s10592-008-9781-0

Hallam A., & Wignall, P. B. (1999). Mass extinctions and sea-level changes. *Earth-Science Reviews*, *48*(4), 217–250. http://dx.doi.org/10.1016/s0012-8252(99)00055-0

Hartl, L. D., & Clark, G. A. (1997). *Principles of Population Genetics (Third Edit)*. Sinauer Associates, Sunderland MA. https://archive.org/details/B-001-001-062/mode/2up

He T., Banerjee A. K., Wu H., He D., Lin Y., Tan F., Tan G., & Huang Y. (2021). Moving past barriers — Sea-drifted seeds shape regional distribution of genetic diversity of a coastal legume in the Indo-West Pacific. *Regional Studies in Marine Science*, *45*, 101861. http://dx.doi.org/10.1016/j.rsma.2021.101861

He, Z., Li, X., Ling, S., Fu, Y.-X., Hungate, E., Shi, S., & Wu, C.-I. (2013). Estimating DNA polymorphism from next generation sequencing data with high error rate by dual sequencing applications. *BMC Genomics*, *14*(1), 535. https://doi.org/10.1186/1471-2164-14-535

He, Z., Li, X., Yang, M., Wang, X., Zhong, C., Duke, N. C., Wu, C.-I., & Shi, S. (2019). Speciation with gene flow via cycles of isolation and migration: insights from multiple mangrove taxa. *National Science Review*, *6*(2), 275–288. https://doi.org/10.1093/nsr/nwy078

Huang, Y., Tan, F., Su, G., Deng, S., He, H., & Shi, S. (2008). Population genetic structure of three tree species in the mangrove genus *Ceriops* (Rhizophoraceae) from the Indo West Pacific. *Genetica*, *133*(1), 47–56. https://doi.org/10.1007/s10709-007-9182-1

Huang, Y., Zhu, C., Li, X., Li, X., Hu, L., Tan, F., Zhou, R., & Shi, S. (2012). Differentiated population structure of a genetically depauperate mangrove species *Ceriops tagal* revealed by both Sanger and deep sequencing. *Aquatic Botany*, *101*, 46–54. https://doi.org/10.1016/j.aquabot.2012.04.001

Hubisz, M. J., Falush, D., Stephens, M., & Pritchard, J. K. (2009). Inferring weak population structure with the assistance of sample group information. *Molecular Ecology Resources*, *9*(5), 1322–1332. https://doi.org/10.1111/j.1755-0998.2009.02591.x

Hudson, R. R. (2002). Generating samples under a Wright-Fisher neutral model of genetic variation. *Bioinformatics*, *18*(2), 337–338. https://doi.org/10.1093/bioinformatics/18.2.337

Kadereit, J. W., Arafeh, R., Somogyi, G., & Westberg, E. (2005). Terrestrial growth and marine dispersal? Comparative phylogeography of five

coastal plant species at a European scale. *Taxon*, *54*(4), 861–876. https://doi.org/10.2307/25065567

Lessios H. A. (2008). The Great American Schism: Divergence of Marine Organisms After the Rise of the Central American Isthmus. *Annual Review of Ecology, Evolution, and Systematics*, *39*(1), 63–91. http://dx.doi.org/10.1146/annurev.ecolsys.38.091206.095815

Li, H., Ruan, J., & Durbin, R. (2008). Mapping short DNA sequencing reads and calling variants using mapping quality scores. *Genome Research*, *18*(11), 1851–1858. https://doi.org/10.1101/gr.078212.108

Li, J., Yang, Y., Chen, Q., Fang, L., He, Z., Guo, W., Qiao, S., Wang, Z., Guo, M., Zhong, C., Zhou, R., & Shi, S. (2016). Pronounced genetic differentiation and recent secondary contact in the mangrove tree *Lumnitzera racemosa* revealed by population genomic analyses. *Scientific Reports*, *6*(1), 29486. https://doi.org/10.1038/srep29486

Librado, P., & Rozas, J. (2009). DnaSP v5: A software for comprehensive analysis of DNA polymorphism data. *Bioinformatics*, *25*(11), 1451–1452. https://doi.org/10.1093/bioinformatics/btp187

Lin Y., Banerjee A. K., Wu H., Tan F., Feng H., Tan G., Guo W., & Huang Y. (2020). Prominent genetic structure across native and introduced ranges of Pluchea indica, a mangrove associate, as revealed by microsatellite markers. *Journal of Plant Ecology*, *13*(3), 341–353. http://dx.doi.org/10.1093/jpe/rtaa022

Liu X., & Fu Y. - X. (2020). Stairway Plot 2: demographic history inference with folded SNP frequency spectra. *Genome Biology*, *21*(1), http://dx.doi.org/10.1186/s13059-020-02196-9

Mamuris Z., Stoumboudi M. T. H., Stamatis C., Barbieri R., & Moutou K. A. (2005). Genetic variation in populations of the endangered fish Ladigesocypris ghigii and its implications for conservation. *Freshwater Biology*, *50*(9), 1441–1453. http://dx.doi.org/10.1111/j.1365-2427.2005.01410.x

Manni, F., Guérard, E., & Heyer, E. (2004). Geographic patterns of (genetic, morphologic, linguistic) variation: how barriers can be detected by using Monmonier's algorithm. *Human Biology*, 173–190. https://doi.org/10.1353/hub.2004.0034

Miller, K. G., Kominz, M. A., Browning, J. V., Wright, J. D., Mountain, G. S., Katz, M. E., & Pekar, S. F. (2005). The Phanerozoic record of global sea-level change. *Science*, *310*(5752), 1293–1298. https://doi.org/10.1126/science.1116412

Minobe, S., Fukui, S., Saiki, R., Kajita, T., Changtragoon, S., Ab Shukor, N. A., Latiff, A., Ramesh, B. R, Koizumi, O., & Yamazaki, T. (2010). Highly differentiated population structure of a Mangrove species, *Bruguiera gymnorhiza* (Rhizophoraceae) revealed by one nuclear GapCp and one chloroplast intergenic spacer trnF–trnL. *Conservation Genetics*, *11*(1), 301–310. https://doi.org/10.1007/s10592-009-9806-3

Molins A., Mayol M., & Rosselló J. A. (2009). Phylogeographical structure in the coastal speciesSenecio rodriguezii(Asteraceae), a narrowly distributed endemic Mediterranean plant. *Journal of Biogeography*, *36*(7), 1372–1383. http://dx.doi.org/10.1111/j.1365-2699.2009.02108.x

Mori, G. M., Zucchi, M. I., & Souza, A. P. (2015). Multiple-geographic-scale genetic structure of two mangrove tree species: the roles of mating system, hybridization, limited dispersal and extrinsic factors. *PLoS One*, *10*(2), e0118710. https://doi.org/10.1371/journal.pone.0118710

Moum, T., & Árnason, E. (2001). Genetic diversity and population history of two related seabird species based on mitochondrial DNA control region sequences. *Molecular Ecology*, *10*(10), 2463–2478. https://doi.org/10.1046/j.0962-1083.2001.01375.x

Nei, M. (1987). *Molecular evolutionary genetics*. Columbia University Press. https://doi.org/10.7312/nei-92038

Nei, M., & Li, W.-H. (1979). Mathematical model for studying genetic variation in terms of restriction endonucleases. *Proceedings of the National Academy of Sciences of the United States of America*, *76*(10), 5269–5273. https://doi.org/10.1073/pnas.76.10.5269

Ngeve, M. N., Van der Stocken, T., Menemenlis, D., Koedam, N., & Triest, L. (2017). Hidden founders? Strong bottlenecks and fine-scale genetic structure in mangrove populations of the Cameroon Estuary complex. *Hydrobiologia*, *803*(1), 189–207. https://doi.org/10.1007/s10750-017-3369-y

Nybom, H., & Bartish, I. V. (2000). Effects of life history traits and sampling strategies on genetic diversity estimates obtained with RAPD markers in plants. *Perspectives in Plant Ecology, Evolution and Systematics*, *3*(2), 93–114. https://doi.org/10.1078/1433-8319-00006

Parks, D. H., Porter, M., Churcher, S., Wang, S., Blouin, C., Whalley, J., … & Beiko, R. G. (2009). GenGIS: a geospatial information system for genomic data. *Genome Research*, *19*, 1896–1904. https://doi.org/10.1101/gr.095612.109

Paulay, G. (1990). Effects of late Cenozoic sea-level fluctuations on the bivalve faunas of tropical oceanic islands. *Paleobiology*, 415–434. https://doi.org/10.1017/S0094837300010162

Pil, M. W., Boeger, M. R. T., Muschner, V. C., Pie, M. R., Ostrensky, A., & Boeger, W. A. (2011). Postglacial north-south expansion of populations of *Rhizophora mangle* (Rhizophoraceae) along the Brazilian coast revealed by microsatellite analysis. *American Journal of Botany*, *98*(6), 1031–1039. https://doi.org/10.3732/ajb.1000392

Pritchard, J. K., Stephens, M., & Donnelly, P. (2000). Inference of population structure using multilocus genotype data. *Genetics*, *155*(2), 945–959. https://doi.org/10.1093/genetics/155.2.945

Rosenberg N. A. (2003). Distruct: a program for the graphical display of population structure. *Molecular Ecology Notes*, *4*(1), 137–138. http://dx.doi.org/10.1046/j.1471-8286.2003.00566.x

Takayama, K., Tamura, M., Tateishi, Y., Webb, E. L., & Kajita, T. (2013). Strong genetic structure over the American continents and transoceanic dispersal in the mangrove genus *Rhizophora* (Rhizophoraceae) revealed by broad-scale nuclear and chloroplast DNA analysis. *American Journal of Botany*, *100*(6), 1191–1201. https://doi.org/10.3732/ajb.1200567

Thornhill, D. J., Mahon, A. R., Norenburg, J. L., & Halanych, K. M. (2008). Open-ocean barriers to dispersal: A test case with the Antarctic Polar Front and the ribbon worm *Parborlasia corrugatus* (Nemertea: Lineidae). *Molecular Ecology*, *17*(23), 5104–5117.

Tomlinson, P. B. (2016). *The Botany of Mangroves*, (2nd Edition). Cambridge University Press. https://lccn.loc.gov/2016015459

Tsuchida, K., Kudô, K., & Ishiguro, N. (2014). Genetic structure of an introduced paper wasp, *Polistes chinensis* antennalis (Hymenoptera, Vespidae) in New Zealand. *Molecular Ecology*, *23*(16), 4018–4034. https://doi.org/10.1111/mec.12852

Urashi, C., Teshima, K. M., Minobe, S., Koizumi, O., & Inomata, N. (2013). Inferences of evolutionary history of a widely distributed mangrove species, *Bruguiera gymnorrhiza*, in the Indo-West Pacific region. *Ecology and Evolution*, *3*(7), 2251–2261.

Venables, W. N., & Ripley, B. D. (2013). *Modern applied statistics with S-PLUS*. Statistics and Computing, 2nd ed. New York: Springer Science & Business Media. https://doi.org/10.1007/978-1-4757-2719-7

Voris, H. K. (2000). Maps of Pleistocene sea levels in Southeast Asia: shorelines, river systems and time durations. *Journal of Biogeography*, *27*, 1153–1167. https://doi.org/10.1046/j.1365-2699.2000.00489.x

Wang, Z., Guo, Z., Zhong, C., Lyu, H., Li, X., Duke, N. C., & Shi, S. (2021). Genomic variation patterns of subspecies defined by phenotypic criteria: Analyses of the mangrove species complex, Avicennia marina. *Journal of Systematics and Evolution*. https://doi.org/10.1111/jse.12709

Wee, A. K. S., Noreen, A. M. E., Ono, J., Takayama, K., Kumar, P. P., Tan, H. T. W., & Webb, E. L. (2020). Genetic structures across a biogeographical barrier reflect dispersal potential of four Southeast Asian mangrove plant species. *Journal of Biogeography*, *47*(6), 1258–1271. https://doi.org/10.1111/jbi.13813

Wee, A. K. S., Takayama, K., Asakawa, T., Thompson, B., Sungkaew, S., & Webb, E. L. (2014). Oceanic currents, not land masses, maintain the genetic structure of the mangrove Rhizophora mucronata Lam. (Rhizophoraceae) in Southeast Asia. *Journal of Biogeography*, *41*(5), 954–964. https://doi.org/10.1111/jbi.12263

Westberg, E., & Kadereit, J. W. (2009). The influence of sea currents, past disruption of gene flow and species biology on the phylogeographical structure of coastal flowering plants. *Journal of Biogeography*, *36*(7), 1398–1410. https://doi.org/10.1111/j.1365-2699.2008.01973.x

Woodroffe C. D., & Grindrod J. (1991). Mangrove Biogeography: The Role of Quaternary Environmental and Sea-Level Change. *Journal of Biogeography*, *18*(5), 479. http://dx.doi.org/10.2307/2845685

Wright, S. (1950). Genetical structure of populations. *Nature*, *166*(4215), 247–249.

Yan, Y.-B., Duke, N. C., & Sun, M. (2016). Comparative analysis of the pattern of population genetic diversity in three Indo-west Pacific *Rhizophora* mangrove species. *Frontiers in Plant Science*, *7*, 1434. https://doi.org/10.3389/fpls.2016.01434

Yang, H., Lu, Q., Wu, B., & Zhang, J. (2012). Seed dispersal of East Asian coastal dune plants via seawater – short and long distance dispersal. *Flora - Morphology, Distribution, Functional Ecology of Plants*, *207*(10), 701–706. https://doi.org/10.1016/j.flora.2012.08.001

Yang, Y., Duke, N. C., Peng, F., Li, J., Yang, S., Zhong, C., Zhou, R., & Shi, S. (2016). Ancient Geographical Barriers Drive Differentiation among Sonneratia caseolaris Populations and Recent Divergence from S. lanceolata. *Frontiers in Plant Science*, *7*, https://doi.org/10.3389/fpls.2016.01618

Yang, Y., Li, J., Yang, S., Li, X., Fang, L., Zhong, C., & Shi, S. (2017). Effects of Pleistocene sea-level fluctuations on mangrove population dynamics: a lesson from *Sonneratia alba*. *BMC Evolutionary Biology*, *17*(1), 22. https://doi.org/10.1186/s12862-016-0849-z

Zachos, J., Pagani, M., Sloan, L., Thomas, E., & Billups, K. (2001). Trends, rhythms, and aberrations in global climate 65 Ma to present. *Science*, *292*(5517), 686–693.

Zhou, R., Qiu, S., Zhang, M., Guo, M., Chen, S., & Shi, S. (2010). *Sonneratia ovata* Backer–A genetically depauperate mangrove species. *Biochemical Systematics and Ecology*, *38*(4), 697–701. https://doi.org/10.1016/j.bse.2010.04.012

SUPPORTING INFORMATION

Additional supporting information may be found in the online version of the article at the publisher's website.

How to cite this article: Zhang, R., Guo, Z., Fang, L., Zhong, C., Duke, N. C., & Shi, S. (2022). Population subdivision promoted by a sea-level-change-driven bottleneck: A glimpse from the evolutionary history of the mangrove plant *Aegiceras corniculatum*. *Molecular Ecology*, 31, 780–797. https://doi.org/10.1111/mec.16290